August 2005

RNA-Activated Protein Kinase, PKR

Yumiko Kobayashi
University of Connecticut

RNA-activated protein kinase, PKR

Honors Thesis

Yumiko Kobayashi

Research Advisor: Dr. James L. Cole
Honors Advisor: Dr. Lawrence Hightower
Spring 2005

Acknowledgements

First and foremost, I would like to thank Dr. James Cole for granting me with such an exciting research opportunity in his lab and for teaching and guiding me through this project. Dr. Cole had tremendous understanding for my inflexible schedule. I would also like to thank Jason Ucci, who taught me various techniques from pipetting to analytical ultracentrifugation. I also thank Peter Lemaire, who led me to successful mutagenesis. I cannot thank enough for both graduate students who helped me to understand the background and general ideas of each experiments. Since I am a part-time student and a mother of two children, I could not have done so many experiments without their support. Their help and encouragement brought me here today. I thank Jeffrey Lary for giving me good advice on analytical ultracentrifuge experiments. I am also thankful for Dr. Alexandrescu for facilitating my project with NMR. Finally, I would like to thank my family. My children, Maho and Kouta, have been very patient while they were waiting for my experiment to be done often outside of the lab and just being good children who help mom very much at home. I need to thank my multitasking husband, Masaru, who was also my scientific writing adviser who cooks, drives kids and goes grocery shopping, for his support and encouragement.

Contents

Results

R.1 Cloning the p10a gene into the pET-11a plasmid
R.2 Optimizing expression of p10a by induction
R.3 Column Chromatography and SDS gel analysis
R.4 Characterizing the oligomeric state of p10a
    4-1 Sedimentation velocity
    4-2 RNA binding stoichiometry
    4-3 Nuclear Magnetic Resonance
    4-4 Circular Dichroism Spectroscopy
R.5 Characterizing the binding of T16E p10a to a dsRNA
    5-1 Mutagenesis – T16E p10a
    5-2 Sedimentation equilibrium

Discussion

D.1. The p10a expression
D.2. The p10a purification
D.3 The p10a binding to dsRNA characteristics

References

List of figures

Abstract

The double-stranded RNA (dsRNA) activated protein kinase, PKR, is one of the several enzymes induced by interferons and a key molecule mediating the antiviral effects of interferons. PKR contain an N-terminal, double-stranded RNA binding domain (dsRBD), which has two tandem copies of the motifs (dsRBM I and dsRBM II). Upon binding to viral dsRNA, PKR is activated via autophosphorylation. Activated PKR has several substrates; one of the examples is eukaryotic translation initiation factor 2 (eIF2a). The phosphorylation of eIF2a leads to the termination of cell growth by inhibiting protein synthesis in response to viral infection. The objective of this project was to characterize the dsRBM I and define the dsRNA binding using biophysical methods. First, the dsRBM I gene was cloned from a pET-28b to a pET-11a expression plasmid. N-terminal poly-histidine tags on pET-28b are for affinity purification; however, these tags can alter the structure and function of proteins, thus the gene of dsRBM I was transferred into the plasmid without tags (pET-11a) and expressed as a native protein. The dsRBM I was transformed into and expressed by Rosetta DE3plyS expression cells. Purification was done by FPLC using a Sepharose IEX ion exchange followed by Heparin affinity column; yielding pure protein was assayed by PAGE.

Analytical Ultracentrifugation, Sedimentation Velocity, was used to characterize free solution association state and hydrodynamic properties of the protein. The slight decrease in S-value with concentration is due to the hydrodynamic non-ideality. No self association was observed. The obtained molecule weight was 10,079 Da. The calculated sedimentation constant at zero concentration at 20°C in water was 1.23 and its friction coefficient was 3.575×10^{-8}. The frictional ratio of sphere and dsRBM I became 1.30. Therefore, dsRBM I must be non-globular and more asymmetric shape.

Isolated dsRBM I exhibits the same tertiary fold as compared to context in the full domain but it exhibited weaker binding affinity than full domain to a 20 bp dsRNA. However, when the conditions allowed for its saturation, dsRBM I to 20 bp dsRNA has similar stoichiometry as full dsRBD.

Introduction

I.1 Double-Stranded RNA binding protein

Molecule recognition of double-stranded RNA (dsRNA) has a critical role in numerous cell regulatory processes, such as trafficking, editing, maturating of cellular RNA, interferon antiviral response, and RNA interference. Although proteins involved in the molecular recognition of dsRNA have varying functions and can identify their specific dsRNA targets, they have structural similarities. Large and diverse classes of proteins that bind to dsRNA do so by utilizing a 65-75 amino acid dsRNA binding motif (dsRBM) and all of the dsRNA binding protein family members possess at least one copy of the dsRBM with which to identify dsRNA (Fierro-Monti *et al.,* 2000). These proteins can have multiple copies of the dsRBMs, which compose a dsRNA-binding domain (dsRBD). The study of protein-dsRNA binding may be helpful to find the way to control the functions of those dsRNA-binding proteins. However, a fundamental understanding of the protein-dsRNA recognition and binding selectivity is currently being established.

There are at least nine families of functionally diverse proteins containing one or more dsRBMs and currently the list of homologous sequences is over 100 that are present in proteins from different organisms, including viruses, bacteria and lower and higher eukaryotes.

I.2 RNA-activated protein kinase, PKR

Interferons are cellular proteins with antiviral activity secreted by vertebrate cells in response to virus infection or antigen stimulation. Healthy cells do not synthesize detectable amounts of interferon and formation of interferons must be induced. Interferons are produced by virus-infected cells to protect uninfected cells against infection or to decrease the chance that virus infection will be able to initiate a productive multiplication cycle in them. Interferons can interact with non-infected cells and induce in these cells an antiviral state; therefore, replication of virus is blocked in interferon-treated cells (Joklik *et al.,* 1988).

The dsRNA activated protein kinase (PKR) is one of several enzymes induced by interferons and is one of the key molecules mediating the antiviral effects of interferons (Stark *et al.,* 1998). It plays a central role in the biological activity of interferons, which are widely employed in the treatment of cancer and viral infections. The importance of this antiviral pathway is highlighted by the diverse mechanisms that viruses have evolved to combat PKR (Gale *et al.,* 1998). A high proportion (60 ~ 80 %) of hepatitis C patients fails to respond to or suffers relapses after interferon therapy. The cause of hepatitis C resistance to interferon has been identified as a viral protein that directly inhibits PKR. Interferon therapy is also not successful against HIV because this virus uses multiple mechanisms to counteract PKR. Thus, the therapeutic effectiveness of interferons is compromised by disease specific resistance and by side effects, including fever, mood disorders, and fatigue. Interferon activates a large number of signaling pathways; therefore, selective activation of one therapeutically relevant component, such as PKR, may lead to reduced side effects and improved clinical outcomes. Direct regulation of

PKR activity may provide an effective way of inducing therapeutic apoptosis in infected or malignant cells. A detailed understanding of the mechanism of PKR activation is required to effectively target this enzyme for clinical intervention against cancer and viral infections.

PKR is synthesized in an inactive state, but upon binding to dsRNA it becomes autophosphorylated and capable of phosphorylating other proteins. There is a new discovery in Cole's lab that PKR can become autophosphorylated in the absence of dsRNA; the reaction is induced by self-association (Lemaire *et al*., 2005). Although self-association of unphosphorylated PKR is weak, this discovery may open new approaches to investigate the PKR activation process. Phosphorylated PKR can phosphorylate eukaryotic initiation factor 2 (eIF2α), thus blocks protein synthesis. Therefore, production of dsRNA during viral infection leads to PKR activation and inhibition of viral protein synthesis. The dsRBMs of PKR are similar to a molecular switch that regulates its kinase activity (Carlson *et al*., 2003). However, several viruses have evolved RNAs that can bind to PKR and block activation of the kinase, in doing so they can avoid the cell's endogenous antiviral response. As a result, PKR has two classes of RNA ligands; kinase activating and kinase inhibiting (Conrad *et al*., 2001). Despite extensive investigations, the features that distinguish RNAs that activate from those that fail to activate remain poorly understood. Development of structure-function relationships of RNA activators will provide a rational basis for the design of drugs to specifically modulate the function of PKR. In addition, studies of dsRNA-independent activation may lead to methods to circumvent inhibition of PKR by kinase inhibiting RNA ligands.

Human PKR is a large protein consisting of 551 amino acids. The N-terminal region is the dsRNA binding domain and the C-terminal region is the kinase domain (Figure 1). The RNA binding domain contains two copies of a 90 amino acid dsRBM labeled dsRBM I and dsRBM II. Studies with truncated PKR proteins show that dsRBM I (p10a) is capable of independently binding to dsRNA (Tian *et al.,* 2001). The second motif (p10b) binds RNA much more weakly.

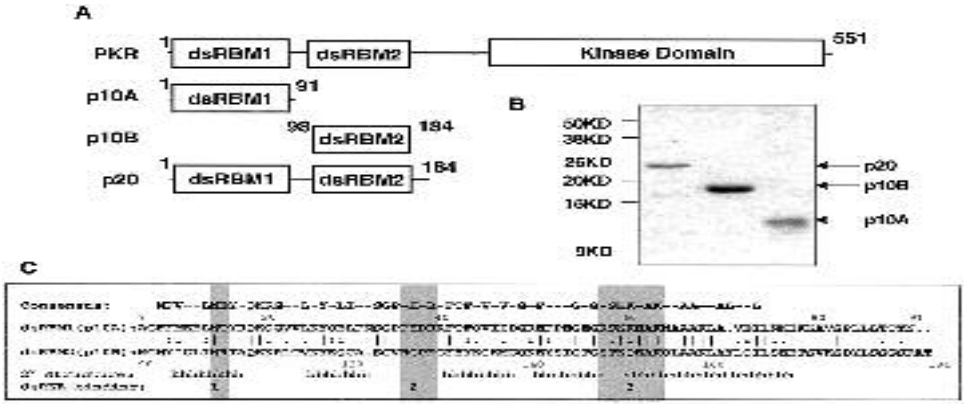

Figure 1 Structure of PKR (Tian *et al*., 2000)

I.3. Why study dsRBM I binding?

A fundamental understanding of the protein-dsRNA recognition and binding selectivity is currently being established and the study of protein-dsRNA binding is helpful to find the way to control the functions of those dsRNA-binding proteins. The selective activation of signaling pathways may lead to improvement in clinical application against cancer and viral infections. Direct regulation of PKR activity may provide an effective way of inducing therapeutic apoptosis in infected or malignant cells. A detailed understanding of the mechanism of PKR activation is required to effectively

target this enzyme. The dsRBMs play a key role in PKR function and regulation, although their exact role in PKR activation is not clear yet.

The study of an isolated dsRBM I is important for promoting better understanding of PKR-RNA binding mechanism. In Cole's lab, studies of the dsRBD-RNA interaction have been pursued earlier (Ucci et al., 2004). The dsRBD binds to dsRNA as one object, thus the role of each of the two dsRBMs in binding cannot be seen. Studies of the interaction of isolated dsRBM I with dsRNA would give a more detailed understanding. Also, the stoichiometry for binding of the dsRBD to a 20 bp dsRNA does not agree with published binding models, which has lead to a new overlapping lattice model of dsRBD-RNA binding (Ucci et al., 2004). In order to test this model, characterization of the simpler dsRBM I-dsRNA interaction is necessary.

I.4 Structural Studies with Affinity Cleavage

In order to clarify the differences between activating and inhibiting PKR-RNA complex, affinity cleavage data have been generated to define the contribution of each of the dsRBMs upon binding dsRNA. Mutations are introduced to control PKR binding strength to dsRNA in each dsRBM by altering its amino acid side chains. The affinity cleavage technique is originally developed as a tool to study DNA binding proteins. The principle of the method is to elucidate specific structural elements using the cleavage pattern of altered point mutations. The point mutations are designed to change the strength of protein-dsRNA bindings. It is widely used to define structural features of complexes between proteins and nucleic acids. In a typical experiment, a hydroxyl radical generator, Fe·EDTA, is site-specifically and covalently attached to a nucleic acid

binding protein, then the hydroxyl radicals are generated which locally cleave the nucleic acid. Finally, this cleavage pattern is mapped onto the dsRNA sequence. The resulting data map is used to define structural elements that determine binding selectivity, such as the number of binding sites present on the nucleic acid, the location of the binding sites, the orientation of the protein on the nucleic acid, and cooperativity of multiple protein motifs.

I.5 Two binding mechanisms of dsRBMs

In Beal's laboratory, the dsRBD was modified with cysteine residue that can conjugate with bromoacetyl-Fe·EDTA at three positions, which are D38C and E29C of dsRBM I and Q120C of dsRBM II (Spanggord *et al*., 2002). The affinity cleavage data were used to create models for the complexes formed by juxtaposing the modified site of the protein with the cleaved nucleotides in the RNA. The inhibiting RNA is derived from the Epstein Barr Virus (EBER 1) and the activating RNA is derived from HIV TAR. With multiple modifications on a single motif, it is possible to establish the orientation and approximate position.

In case of an inhibiting RNA, only dsRBM I binds to the dsRNA at two distinct sites but dsRBM II does not bind to the dsRNA at all. The inhibiting RNA only interacts with the dsRBM I, allowing the dsRBM II to inhibit the kinase domain of PKR (Vuyisich *et al.,* 2002). It seems as if the viral RNA is designed to sequester two equivalents of PKR in an inactive state to support viral proliferation.

In contrast, in the case of an activating RNA, both dsRBM I and dsRBM II bind to the distinctive sites on the same RNA ligand simultaneously (Figure 2). It appears that

simultaneous binding to TAR relieves the inhibitory contacts to the kinase domain and supports activation of protein. These data agree with the observations that longer duplex regions are required for PKR activation, although only 16-18 bp is sufficient to support binding of one dsRBM of PKR.

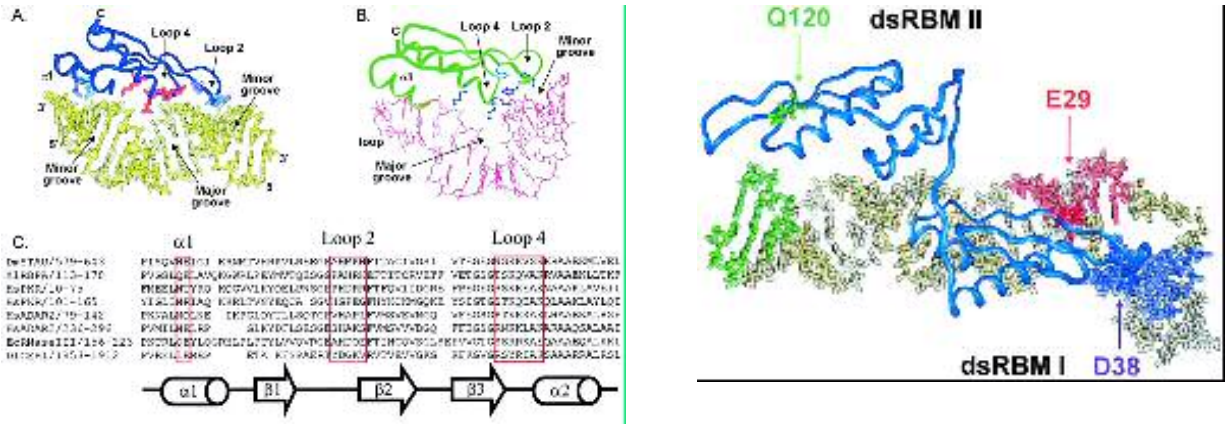

Figure 2**: A**. Crystal structure of the *X. laevis* RNA binding protein A (Xlrbpa) bound to dsRNA. Three regions on the RNA contacted by dsRBM (Ryter and Schultz, 1998). **B**. NMR structure of Staufen's third dsRBM bound to a stem-loop RNA (Ramos *et al.*, 2000). **C**. Sequence alignment of numerous dsRBMs. **D**. Model of HIV TAR RNA binding with PKR (Spanggord and Beal *et al.,* 2003)

The cleavage pattern with kinase – activating RNA supports two binding sites for dsRBM I and one binding site for dsRBM II. The cleavage pattern derived from dsRBM II overlapped with one of the dsRBM I sites, so it seems both motifs do not bind to this site simultaneously. However, the second binding site for dsRBM I could be occupied with simultaneous binding by dsRBM II.

In order to test the dependence of dsRBM I on dsRBM II for binding, a K150A mutation in dsRBM II was introduced to reduce the affinity of dsRBM II. The K150A mutation has been shown to decrease the binding affinity of PKR for RNA (Patel *et al.*, 1996). The mutant protein was labeled with bromoacetyl-Fe·EDTA at dsRBM I. The

two binding sites of dsRBM I are at the 5'-stem loop and 3'-stem loop. The 5'-stem binds to only dsRBM I and 3'-stem may bind to either dsRBM I or dsRBM II. The modified protein shows decreased cleavage at 5'-stem loop. This indicates that the binding of dsRBM I to the 5'-stem loop site is dependent on dsRBM II binding (Spanggord *et al*., 2002). Decreased affinity of dsRBM II to RNA leads also to an increased efficiency of cleavage at the 3'-stem by dsRBM I. For the further investigation of simultaneous binding, RNA concentration was reduced so that only the 3'-stem binding site was occupied. As a result, dsRBM I bound the RNA but dsRBM II did not. Consequently, there are two binding mechanisms observed from above data; the cooperative binding of both motifs in one complex, and independent binding of dsRBM I in a separate protein-RNA complex.

These experiments also address the intrinsic binding selectivity. These dsRBMs may not exhibit strict sequence specificity; however, they clearly have the ability to distinguish distinct structural features of RNA (Carlson *et al*., 2003). The dsRBMs show the ability to bind to known RNA ligands in a site-selective manner. Additionally, the differences of selectivity for binding between two motifs are observed. The affinity cleavage data suggest that dsRBMs do not bind to kinase-inhibiting RNA simultaneously and have two distinct binding sites only for dsRBM I but not for dsRBM II. In contrast, the data suggest that both dsRBM I and dsRBM II can bind to kinase-activating RNA simultaneously.

I-6 Sedimentation of Particles in a Gravitational Field

Sedimentation velocity is a useful tool to understand some of the physical characteristics of proteins. Initially uniform protein solution is placed in the cell and very high angular velocity is used to cause rapid sedimentation of the protein toward the cell bottom. This rapid sedimentation produces a depleted region of protein near the meniscus and the formation of sharp boundary between the depleted region and the uniformly sedimenting protein region. The actual velocity of individual protein molecule cannot be measured; however, the rate of movement of the boundary can be measured. The sedimentation coefficient, which is directly related to the mass of the particle and inversely to the friction coefficient, can be found in this experiment. When a protein (solute) is suspended in a buffer (solvent) and high angular velocity is applied, three forces act on the protein;

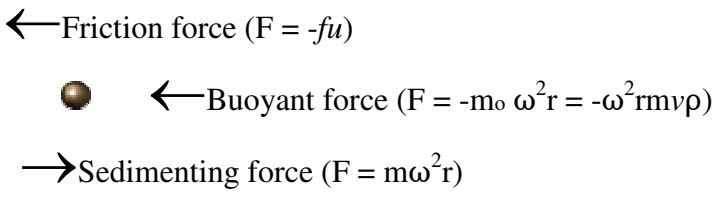

There is a sedimenting force (gravitational force), F, which is proportional to the mass of the particle and the acceleration. The acceleration is determined by the distance of the particle from the axis of rotation, r, and the square of the angular velocity, ω.

$$\mathbf{F = m\omega^2 r = (M\omega^2 r) / N_A} \qquad ①$$

where m is the mass (g) of a single particle, M is the molar weight of the solute (g/mol) and N_A is Avogadro's number.

There is also a buoyant force (F_b), which can be explained by Archimedes' principle. And it is equal to the weight of fluid displaced:

$$\mathbf{F = - m_o \omega^2 r} \qquad ②$$

where m_o is the mass of fluid displaced by the particle:

$$\mathbf{m_o = m\ \rho = (M\nu\rho) / N_A} \qquad ③$$

where ν (mL/g) is the partial specificvolume of the protein and ρ (g/mL) is the density of the buffer. When the density of the protein is greater than that of the buffer, the protein will begin to sediment. The protein begins to move along a radial path toward the cell bottom. As the protein moves toward the cell bottom, its velocity, *u*, will increase because its radial distance increases. Because protein is moving through a viscous fluid, it will have a frictional force that is proportional to the velocity;

$$\mathbf{F = -}\mathit{\mathbf{fu}} \qquad ④$$

where *f* is the friction coefficient, which depends on the shape and size of the protein. Asymmetric or elongated proteins have more frictional drag than globular, smooth ones. The equations ② and ④ must have negative signs because these two forces act in the opposite direction from sedimentation force.

When the three forces come into balance:

Friction force + Buoyant force + Sedimenting force = 0 ⑤

$$\mathbf{(M\omega^2 r / N_A) - (M\nu\rho\omega^2 r / N_A) -} \mathit{\mathbf{fu}} \mathbf{= 0} \qquad ⑥$$

$$\mathbf{\{M\omega^2 r\ (1-\nu\rho) / N_A\} -} \mathit{\mathbf{fu}} \mathbf{= 0} \qquad ⑦$$

When the terms that relate to the particle and the terms that relate to the experimental conditions combine:

$$\mathbf{\{M(1-\nu\rho)\omega^2 r\} / N_A} \mathit{\mathbf{f}} \mathbf{= u / \omega^2 r =} \mathit{\mathbf{S}} \qquad ⑧$$

The velocity of the protein per unit gravitational acceleration ($u / \omega^2 r$) is called the *sedimentation coefficient, S*, and it is a physical property of the protein. It is proportional to the buoyant effective molar weight of the protein and it is inversely proportional to the friction coefficient. If the proteins in the buffer have different molecular weights, or different shapes and sizes, they move with different velocities under the application of the same centrifugal field, therefore, each protein will have their own unique sedimentation coefficients. The unit of the sedimentation coefficient is seconds.

Measurement of the rate of sedimenting boundary broadening can be used for determination of the *diffusion coefficient, D*, which is proportional to effective size of the proteins:

$$D = RT / N_A f \qquad ⑨$$

where R is the gas constant and T is the absolute temperature. The ratio of the sedimentation coefficient to the diffusion coefficient gives the molecular weight:

$$M = S^\circ RT / D^\circ (1-v\rho) \qquad ⑩$$

where M is the molar weight of the solute, v is partial specific volume, and ρ is the solvent density. The S° and D° are the values at zero concentration, which are calculated from several measurements at several different concentrations to remove the effects of interaction between proteins on their movement. Approximate molecular weights can be estimated using sedimentation coefficient and diffusion coefficient. The existence of a single sedimenting boundary indicates homogeneity. On the other hand, the existence of multiple boundaries is evidence for multiple sedimenting species.

In cases where a protein undergoes association reactions, the molecular weight of the protein increases. Therefore, the sedimentation coefficient will increase with

increasing protein concentration. The sedimentation pattern will become complex and will depend on the rate of association and dissociation reactions. If the rates of interconversion are slow compared to the time of the sedimentation experiment, each species can give rise to a separate boundary. In this case, the molecular weights, sizes and shapes of the various oligomers can be analyzed.

In order to determine a molecule weight using the sedimentation coefficient, accurate estimation of the diffusion coefficient is necessary. The diffusion coefficient also provides information useful about the size and shape of the solute particles. The frictional coefficient is proportional to the radius, R, of a spherical particle:

$$\mathbf{F = 6\pi\eta R} \qquad 11$$

The friction coefficient increases as the shape diverge from sphere. For ellipsoids, f increases with the axial ratio, and increases more for elongated ellipsoids than for flattened ellipsoids. The frictional ratio is useful in estimating molecule shape. The frictional ratio is a comparison of the measured friction coefficient, f, with a calculated friction coefficient of a smooth sphere model, f_o, assuming that the smooth sphere has the same weight and specific volume. The frictional ratio, f / f_o, has been found to be near 1.2 for globular proteins, and increases with asymmetry.

In sedimentation equilibrium, a small volume of an initially uniform solution is centrifuged at lower angular velocity. As a protein begins to sediment towards the cell bottom, the concentration at the bottom increases. The force of diffusion opposes to the force of sedimentation. After an appropriate period of time, the two forces approach to equilibrium. The concentration of the protein increases exponentially towards the cell

bottom. When it reaches to equilibrium, there is no net movement of molecules, because the diffusion force exactly balances sedimentation force everywhere in the cell.

$$C(r) = C_o \exp[M(1-\nu\rho)\omega^2/2rT(r^2-r_o^2)] \quad (12)$$

where M is the solute molar weight (g/mol), ω is the angular velocity of the rotor, c is the concentration of the solute (g/L) and r is the radial distance from the axis of the rotation. The sedimentation equilibrium is the best way for determining the molecular weight of macromolecule. The radial concentration gradient is determined by the molecular weight of the protein.

To monitor binding of dsRBM I to dsRNA, various concentrations of protein will be tested. As the concentration of protein increases, the probability of protein binding to dsRNA increases. By varying the ratio of protein concentration to dsRNA concentration up to the saturation point, the stoichiometry of protein and dsRNA can be determined. It is a measurement of the increase in the dsRNA buoyant mass in presence of saturating concentration of protein. In order to achieve the stoichiometric binding conditions, the RNA concentration must be significantly higher than the protein-RNA dissociation constant.

Materials and Methods

M.1. Cloning the p10a gene in pET-11a plasmid

1-1 Preparation of plasmids

Originally, the dsRBM I gene received from M. B. Mathews was in a pET-28b expression plasmid. However, the N-terminal poly-histidine tags on pET-28b can alter the structure and function of proteins, thus the gene of dsRBM I was attempt to transfer into the pET-11a expression plasmid, which has no tags. The p10a gene was excised from a pET-28 expression vector using an NdeI restriction site immediately before the start codon and BamHI restriction site after the stop codon. The double digest was incubated at 37 °C overnight but no longer than 16 hrs. Samples from the restriction digestion were desalted and concentrated to approximately 20 μL using a microconcentrifugal filter device, YM10. Samples were purified on a 1.2% weight/volume agarose gel. The DNA was extracted from the gel using UltraFree-DA kit. DNA samples were concentrated to approximately 20 μL using the microconcentrifugal filter device YM10. The insert was cloned into pET-11a to obtain pET-11a p10a. The DNA was sequenced afterwards for confirmation.

a. Preparation of pET-28-p10a

A glycerol stock of pET-28, a kanamycin resistant plasmid containing the p10a gene, was grown in LB medium with 30 μg/mL kanamycin at 37 °C overnight to obtain a

liquid culture. Plasmid DNA was extracted using QIA prep spin Miniprep kit (QIAGEN Science) and the concentration was determined by UV spectroscopy.

b. Confirmation of p10a gene in pET-28 plasmid by ABI-prism sequencing

b-1) DNA dilution

Sample	Stock concentration	Volume taken	Amount of DNA
P10a	125.6 (ng/μL)	10 μL	1256 ng
primer	5 μM (5 pmol/μL)	1 μL	5 pmol

b-2) Reaction Mixture

pure water	1 μL
template DNA	10 μL (1256ng)
T7 primer	1 μL (5 p mol)
Terminator ready reaction mix	8 μL
total	20 μL

b-3) Thermocycling Program

segment	cycle	Reaction	temp(°C)	time
1	1	melting	95	3 min
2	40	melting	95	30 sec
		annealing	50	30 sec
		extension	60	4 min
3		hold	4	indefinitely
	end			

*Mixture was heated in segment 1 for 2 min before adding Big-dye terminator ready reaction mix.

b-4) Ethanol Percipitation of PCR product

Two μL of 3M Sodium acetate (pH 5.2) and 40 μL of cold 95% ethanol (-20 ºC) were added to the PCR product DNA and let it sit for 30 min. The solution was

centrifuged at 14,000rpm for 10 min at 4 ºC. The pellets were washed twice with 150 µL of cold 70% ethanol (-20 ºC) and centrifuged at 14,000 rpm for 10 min at 4 ºC. The tubes were left on the bench overnight to dry.

1-2 Double restriction digestion

PpET-11a

	Stock concentration	Volume added (µL)	Final amount
fsdH_2O	-	126	
React 6	10 X	20	1X
DNA	194.6 ng/µL	40	7.784 µg
BSA	100X (10mg/mL)	2	100 µg/mL
Nde I	5U/µL	8	40U
BamH I	10U/µL	4	40U
Final Volume		200	

-1U of enzyme was required to digest 1 µg of DNA in I hr at 37 °C, hence this represents approximately 5X over digestion.

PET28-p10a

	Stock concentration	Volume added (µL)	Final amount
fsdH_2O	-	411	
React 6	10 X	60	1X
DNA	243.7 ng/µL	90	21.933 µg
BSA	100X (10mg/mL)	6	100 µg/mL
Nde I	5U/µL	22	110U
BamH I	10U/µL	11	110U
Final Volume (µL)		600	

-1U of enzyme was required to digest 1 µg of DNA in I hr at 37 °C, hence this represents approximately 5X over digestion.

1-3 Ligation

The following components were mixed well before adding T4 DNA ligase. The entire mixture was mixed again, spun down and incubated at 16 °C overnight.

components	- control	background	reaction 1	reaction 2
fsdH_2O	8	15	0	0
5X ligase rxn buffer	4	4	4	4
PET-11 a digested	0	2	2	2
P10a insert	0	0	4	10
T4 DNA ligase	1	1	1	1
Final Volume (μL)	20	20	20	20

1-4 Transfer p10a gene

The 1.5 μL ligation mixture was transferred into 50 μL NovaBlue competent cells and 25 μL, 50 μL, and 100 μL of cells were plated on LB plates containing 50 μg/mL carbenicillin. As a control, 1.5 μL of pET-28 was transferred into 25 μL of NovaBlue competent cells were plated. The transformed plates were incubated at 37 °C overnight.

The pET-11a-p10a expression vector was transferred into Rosetta (DE3) pLyS cells for protein expression (Novagen). The transferred gene was confirmed to have no mutation during this procedure by ABI-Prism sequencing. The overnight cultures of six colonies were made and glycerol stocks of them were stored at - 80°C.

M.2. Optimizing expression of p10a

2-1 Preparation prior to the testing induction

500 mL of LB broth was prepared in a 2 L flask by adding 12.5 g of solid LB to mix and was sterilized for 60 min on liquid cycle by autoclaving. After the LB broth was cooled, chloramphenicol (34 μg/mL) and carbenicillin (50 μg/ml) were added. A 5 ml starter culture was inoculated with pET-11a-p10a in Rossetta cells and incubated overnight in the shaker incubator at 37°C at a speed of 250 rpm.

2-2 Induction test

To 500 mL of LB broth in 2 L flask, 3 mL of over night culture was added. Its OD (absorbance) at 600 nm, $A_{600,}$ was measured immediately to find its baseline. The starting culture in 2 L flask was placed in shaker incubator at 37°C and the OD was measured in order to observe the cell growth. When the OD value reached 0.6, isopropyl-β-D-thiogalactopyranoside (IPTG) was added so that the final concentration was 1 mM. The pre-induced and 1, 2, 3 hour induced samples were stored for later gel analysis to characterize p10a induction.

2-3 Gel analysis of induction

a. Preparation prior to the experiment

Samples (120 μL) were thawed and transferred into microtubes. The samples were centrifuged at max speed for 15 min and pellets were resuspended with 120 μL of pure water. Then Trichloroacetic acid (TCA) was added, so that the final concentration of TCA would be 10% (30 μL of 50% TCA solution). The solution was centrifuged for 20 min at max speed. In order to remove TCA, 1 mL of acetone was added without disturbing the pellet then centrifuged for 5 min at max speed. The pellet was dried by removing excess acetone and exposed to air. The pellets were suspended with 35 μL pure water and SDS loading buffer was added so that the final concentration was 25% (12 μL). BME was added, so that the final concentration of BME is 15% (10 μL of 14.2M BME). The solution was vortexed for 30 sec. The solution was heated for 10 min at 70 °C.

b. Running SDS gel

The samples were loaded onto 12% Polyacrylamide precast gels and electrophoresed at 200 V for 40 min. After running, the gel was stained with 500 mL Coomassie Brilliant Blue and heated for 30 sec at high power in a microwave oven. After 15 min of staining, the gel was destained for 15 min. Then the destain solution was discarded and water was added, the gel was heated for 30 sec with high power and placed on the shaker at room temperature for 15 min. After 15 min, water was discarded and fresh water was added to the gel, heated for 30 sec with high power and set for 15 min and it was repeated twice.

M.3 Protein purification

3-1 Cell Lysis

For p10a protein purification, cells were resuspended in buffer A (20 mM Bicine, 50 mM NaCl, 1 mM EDTA, 5% Glycerol, 10 mM β-mercaptoethanol, pH 8.0) supplemented with protease inhibitor cocktail (Sigma). Cells were lysed by sonication for 20 cycles of 30 sec. on ice followed by PEI precipitation by adding 4% PEI solution to the suspended cell lysate to yield a 0.2% w/v final concentration. The lysate was centrifuged for 15 min at 20,000 g.

3-2 Column chromatography

The supernatant was applied to an S-Sepharose ion exchange column (Amersham) equilibrated in buffer A and p10a was eluted using a NaCl gradient from 50 mM to 1 M. The peak fractions were diluted two-fold with buffer A0 (20 mM Bicine, 1 mM EDTA,

5% Glycerol, 10 mM β-mercaptoethanol, pH 8) in order to reduce its salt concentration and applied to a Heparin Sepharose column (Amersham) equilibrated in buffer A. The p10a protein was eluted using the same NaCl gradient, concentrated to approximately 8.52 mg/mL and stored at – 80 °C.

M.4. Characterizing the binding of p10a

4-1 Sedimentation velocity and sedimentation equilibrium

Analytical ultracentrifugation was performed with a Beckman-Coulter XL/I instrument at 20 °C. Samples were equilibrated into analysis buffer (75 mM NaCl, 20 mM Hepes, 0.1 mM EDTA, pH 7.5) using spin columns. The buffer density was measured to be 1.0059 g/mL using an Anton Paar DMA-60 density meter. Protein concentrations were assayed using $A_{280\,nm.}$ The following properties were calculated using Sednterp; ε_{280} in water = 2.980 x 10^{-3} $M^{-1}cm^{-1}$, M = 10,252.73, v-bar = 0.7399 g/mL. Standard 2-channel and external-loading, 6-channel centerpieces were used for sedimentation velocity and equilibrium experiments, respectively. Sedimentation equilibrium data were fit using non-linear least squares fitting algorithms with macros developed in IGOP Pro (Wavemetrics).

4-2 Circular Dichroism Spectroscopy

CD spectra was recorded on a Jasco J-715 spectrometer at 20 °C from 350 to 200 nm with 1 nm spectral bandwidth and 50 nm/min scan rate. CD titration of the 20 base pair dsRNA with p10a was performed at high RNA concentrations of 7 μM, 10 μM and 20 μM. The dsRNA was made by annealing top and bottom strands and its concentration was measured by spectroscopy. The sample was loaded into a 2 mm path length quartz cuvette. Ten scans at 262 nm were averaged for each spectrum. Data were acquired for

the dsRNA alone and following sequential additions from a 126 μM stock of p10a spectra were corrected for dilution effects, and the intensity data was plotted using KaleidaGraph.

20mer dsRNA

```
Bottom strand 20 5′-CGAAGGGCAUGAAGUUCUCC-3′
   Top strand 20 3′-GCUUCCCGUACUUCAAGAGG-5′
```

BS20

Mw = 6405.9 Daltons
Extinction @ 260 nm = $2.26X10^5$ $M^{-1}cm^{-1}$ (by Excel calculator)

TS20

Mw = 6342.8 Daltons
Extinction @ 260nm = $2.16X10^5$ $M^{-1}cm^{-1}$

TS20-BS20 duplex

Mw = 12748.7 Daltons
Extinction @ 260 nm = $3.26X10^5$ $M^{-1}cm^{-1}$ (.739 x T20+B20)
Extinction @ 295 nm = $2.96X10^4$ $M^{-1}cm^{-1}$ (experimental)
V-bar = **.51**
(calculated from experimental buoyant weight and known SB4 density)

4-3 Nuclear Magnetic Resonance, NMR

The overall fold of the p10a protein was assayed by NMR spectra. Protein enriched in ^{15}N was prepared by growing cells minimal media. The MOPS medium was prepared as the established protocol in Alexandrescu lab and enough ^{15}N p10a protein was produced for NMR analysis. The procedure was performed by Dr. Alexandrescu in his laboratory

Recipe of MOPS medium for 300 mL total

260 mL of sterile H_2*
70 mL of 5XM buffer
0.7 mL of O solution
0.7 mL of P solution
0.4 mL of S solution
0.4 mL of 0.1% B1 stock
3.5 mL of 40% glucose
20 mM ^{15}N Ammonium Chloride
(*Add ^{15}N just before induction)

M.5. Characterizing the binding of T16E p10a

5-1 Mutagenesis

a. Primer design and preparation

Introduction of a point mutation at T16E (ACA →GAA), which will change one amino acid at position 16 in dsRBM I.

T16E p10a coding (above) and non-coding (below) primer design

```
5'- GCAGGTTTGTCATGGAGGAACTTAATGAATACCGTCAGAAGCAGGG -3'
3'- CGTCCAAACAGTACCTCCTTGAATTACTTATGGCAGTCTTCGTCCC -5'
```

The concentration of the primers was measured with spectroscopy.
[T16E top] = 630 ng/μL
[T16E bottom] = 823 ng/μL

b. Temperature cycling and Site directed mutagenesis

Site directed mutagenesis was performed using the Quick Change Kit (Stratagene). The plasmid was denatured and annealed with the oligonucleotide primers containing a point mutation at T16E. Using the nonstrand-displacing action of PfuTurbo DNA

polynucrease, the mutagenic primers were extended and incorporated, resulting in nicked circular strands

Reaction mix; The followings were added to the small dome cap micro tube in order;

	<Reaction 1>	**<Reaction 2>**
1) pure water	- 40.7μL	- 35.2 μL
2) 10X reaction buffer	- 5 μL	- 5 μL
3) DMSO (4% of total volume)	- 5 μL	- 5 μL
4) plasmid pET11a-p10a	- 1.5μL = 127.5 ng	- 1 μL
5) T16E top primer	- 1 μL = 630 ng	- 125 ng
6) T16E bottom primer	- 0.8 μL = 658 ng	- 131.6 ng
7) dNTPs	- 1 μ	- 1 μL
Total	- 49μL	- 49 μL

Thermocycling Program

segment	cycle	Reaction	temp(°C)	time
1	1	melting	95	3 min
2	18	melting	95	30 sec
		annealing	55	1 min
		extension	68	14 min
3		hold	4	indefinitely
	end			

*Mixture was heated in segment 1 for 2 min before adding Pfu turbo enzyme

c. Digestion

The completed SDM reaction solution was digested by DpnI restriction enzyme in order to eliminate methylated and wild-type parent DNA template.

d. Ligation

The digested components were mixed well before adding ligase. The entire mixture was mixed again, spun down and incubated at 16 °C overnight.

e. Transfer p10a gene

The ligation product was transformed into 50 μL XL1-Blue supercompent cells. The transformation reactions were swirled gently to mix and incubate the reactions on ice for 30 min. A heat pulse was applied to the transformation reactions for 45 sec. at 42 °C by dipping the tube in 42 °C water bath, and then the reaction was placed on ice for 2 min. Appropriate volumes of cells were plated on the LB plates containing carbenicillin (50 μg/mL). The transformed plates were incubated at 37 °C overnight.

The procedure described in "1-1 Preparation of plasmids" was used to make glycerol stocks in NovaBlue cells and Rosetta (DE3) plysS cells. The glycerol stocks were stored at – 80 °C.

Results

1.Cloning the p10a gene into the pET-11a plasmid

The NovaBlue competent cells, that contain the anpicillin resistant pET-11a plasmid with a p10a gene insertion, produced many colonies on the LB plates containing 50 μg/mL carbenicillin. In contrast, no colonies were observed for the negative control, the NovaBlue competent cells with kanamycin resistant plasmid pET-28, and with background plates lacking the insert. This result indicated the success of p10a gene transfer from the pET-28 plasmid to the pET-11a plasmid. The sequence of the pET-11a plasmid with p10a gene insertion was confirmed by ABI-Prism sequencing. The glycerol stocks of pET-11a p10a in NovaBlue and Rosetta cells were stored for later experiments.

2. Optimizing expression of p10a by induction

The cells were grown in LB medium at 37 °C until $A_{600\ nm}$ approximately 0.6 and optimal protein expression was determined to be three-hour induction with 1 mM IPTG at 37 °C.

Cell Growth at Induction

Time (hr)	0	1.5	2.5	3.5	4	5
$A_{600\ nm}$	0.055	0.021	0.03	0.092	0.247	0.6

It took about four hours to reach 0.3 OD. After reaching to the doubling rate, the cell growth was exponential. Within one hour it reached to the ideal concentration for induction.

MES SDS Gel Analysis of Testing Induction (figure 3)

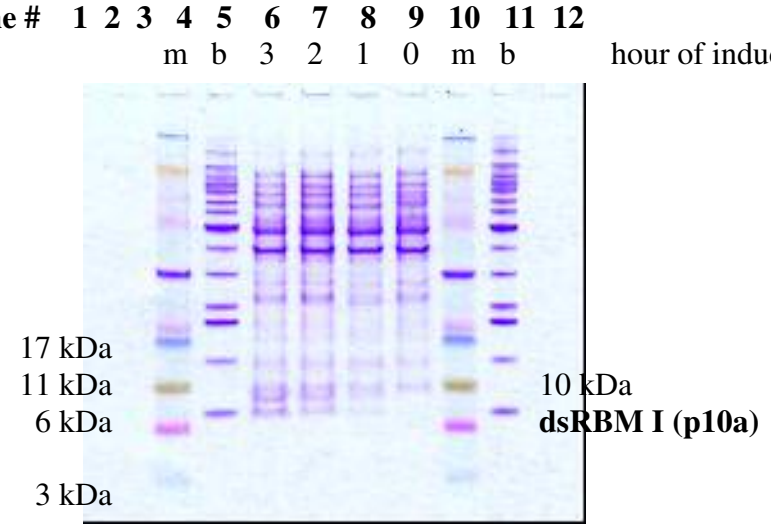

Lane	1	empty
	2	empty
	3	empty
	4	MultiMark 5 uL
	5	Bench marker 5 uL
	6	3-hour induction 30 uL
	7	2-hour induction 30 uL
	8	1-hour induction 30 uL
	9	pre-induction 30 uL
	10	MultiMark 5 uL
	11	Bench marker 5 uL
	12	empty

The gel result showed that three-hour induction had the most p10a production compared to 2hr, 1 hr and pre-induction.

From 500 mL of LB in a 2 L flask, 9.49 mg/Liter of cell paste was protein was harvested.

3 Column Chromatography (figure 4)

▪

The lysed cells were treated by PEI precipitation and centrifugation. The supernatant was applied to an S-Sepharose ion exchange column (Amersham) equilibrated in buffer A and p10a was eluted using a NaCl gradient from 50 mM to 1 M. The peak fractions were diluted two-fold with buffer A0 (20 mM Bicine, 1 mM EDTA, 5% Glycerol, 10 mM β-mercaptoethanol, pH 8) in order to reduce its salt concentration and applied to a Heparin Sepharose column (Amersham) equilibrated in buffer A. The p10a protein was eluted using the same NaCl gradient, concentrated to approximately 8.52 mg/mL and stored at – 80 °C.

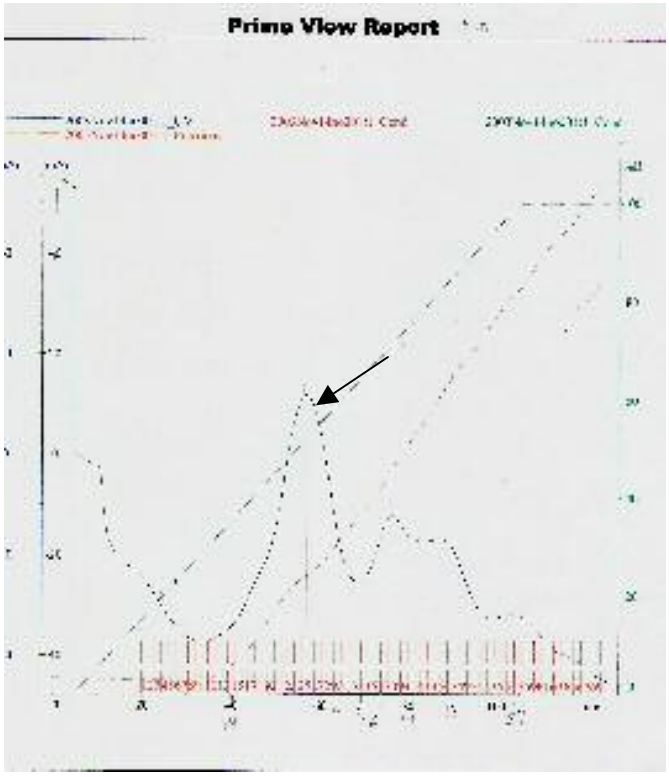

S Sepharose ion exchange column
fraction #46 - #36, #41,#47 and #57 were analyzed by the SDS gel

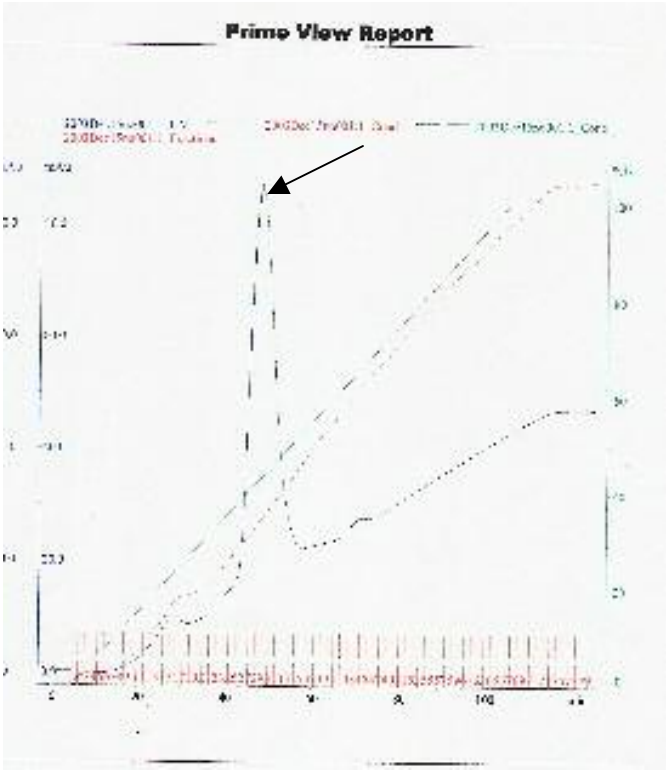

Heparin Sepharose affinity column
fraction #24 - #34 were analyzed by the SDS gel

SDS Gel Analysis of S-Sepharose Protein Purification (Figure 5)

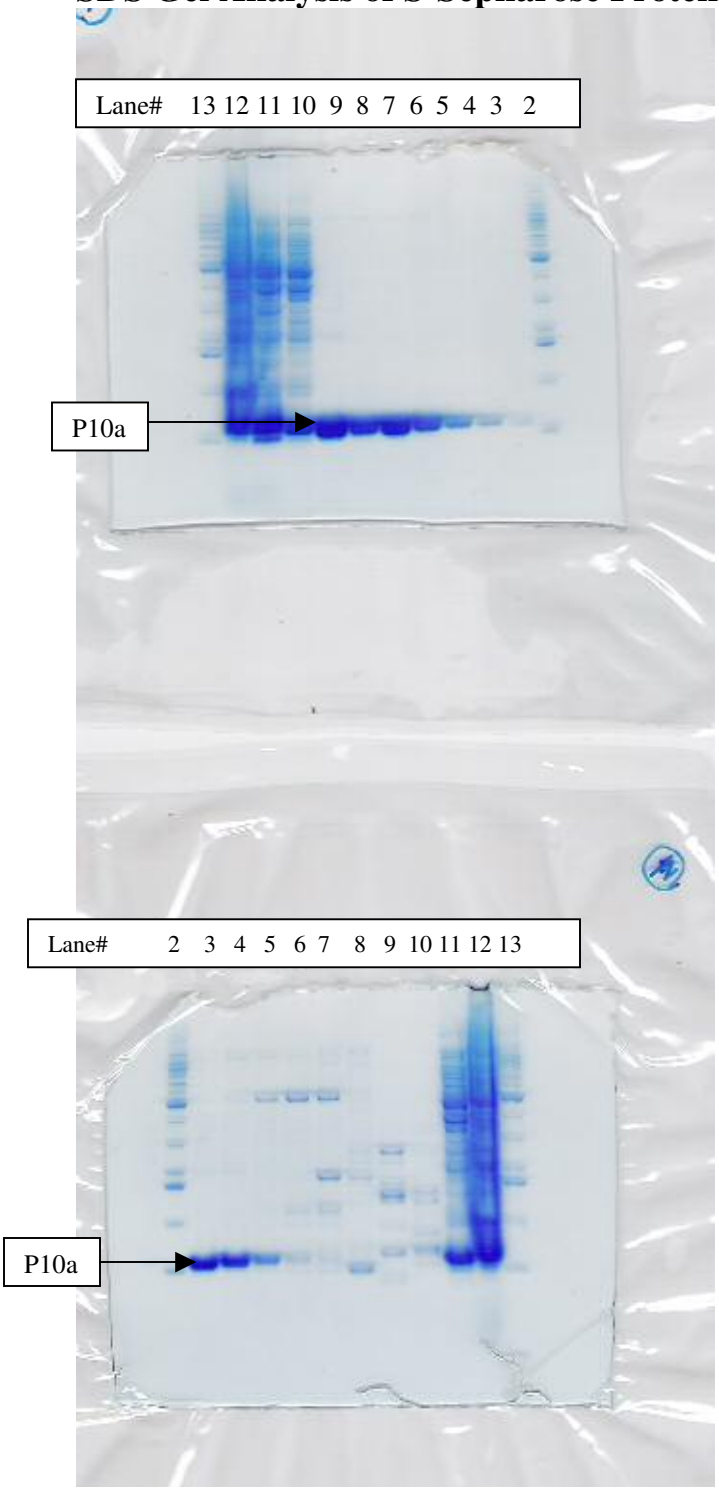

1. empty
2. marker
3. fraction #14
4. fraction #16
5. fraction #18
6. fraction #20
7. fraction #22
8. fraction #24
9. fraction #26
10. flow through
11. PEI precipitate
12. PEI supernatant
13. marker
14. empty
15. empty

1. empty
2. marker
3. fraction #28
4. fraction #30
5. fraction #32
6. fraction #34
7. fraction #36
8. fraction #41
9. fraction #47
10. fraction #57
11. flow through
12. PEI supernatant
13. marker
14. empty
15. empty

These gels were dried instead of being scanned. The lane 9-5 of upper gel, and lane 3 and 4 of bottom gel are demonstrating fairly well purified p10a protein.

SDS Gel Analysis of Heparin Sepharose Column Protein Purification (Figure 6)

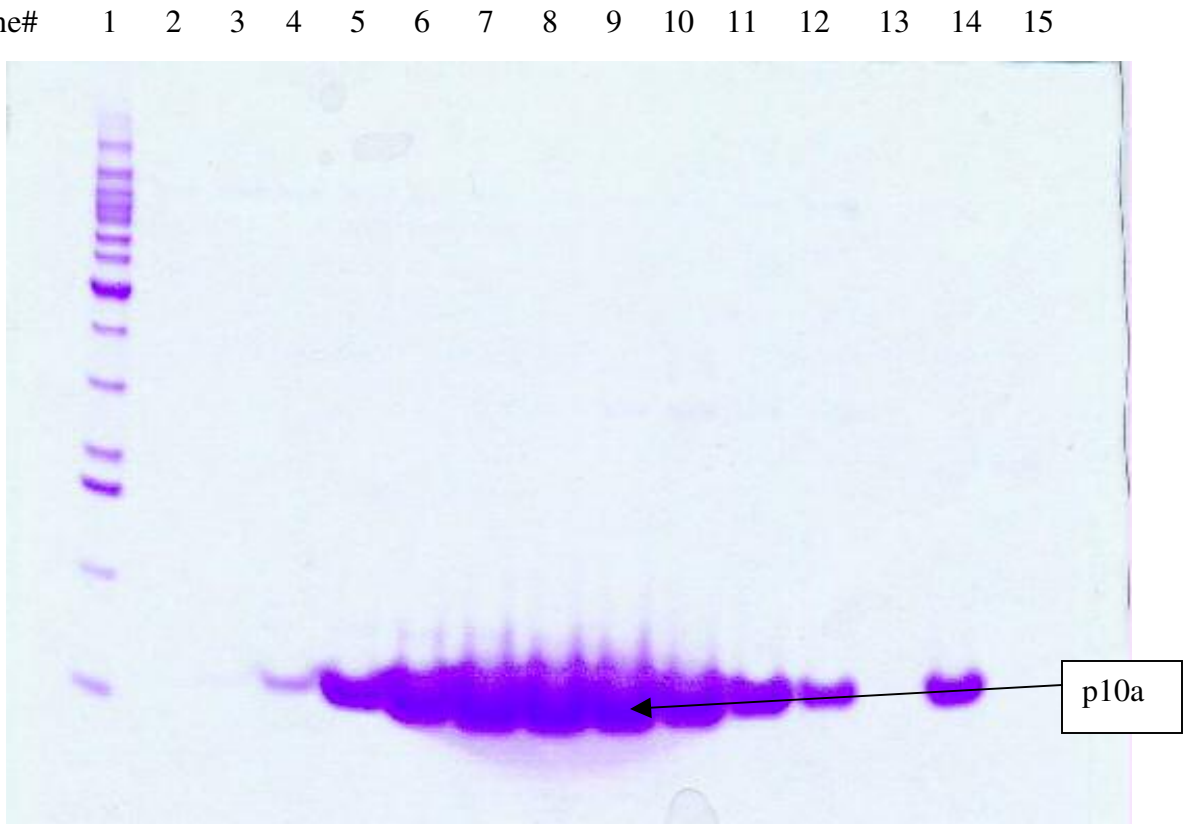

Lane		
	1	marker, 5uL
	2	fraction # 24, 20 µL
	3	fraction # 25, 20 µL
	4	fraction # 26, 20 µL
	5	fraction # 27, 20 µL
	6	fraction # 28, 20 µL
	7	fraction # 29, 20 µL
	8	fraction # 30, 20 µL
	9	fraction # 31, 20 µL
	10	fraction # 32, 20 µL
	11	fraction # 33, 20 µL
	12	fraction # 34, 20 µL
	13	flow through 20 µL
	14	starting material 20 µL
	15	fraction # 15 (contaminant), 20 µL

The heparin Sepharose column was able to complete the purification process of p10a to produce pure p10a.

4. Characterizing the oligomeric state of p10a (Figure 7)

4-1 Sedimentation Velocity

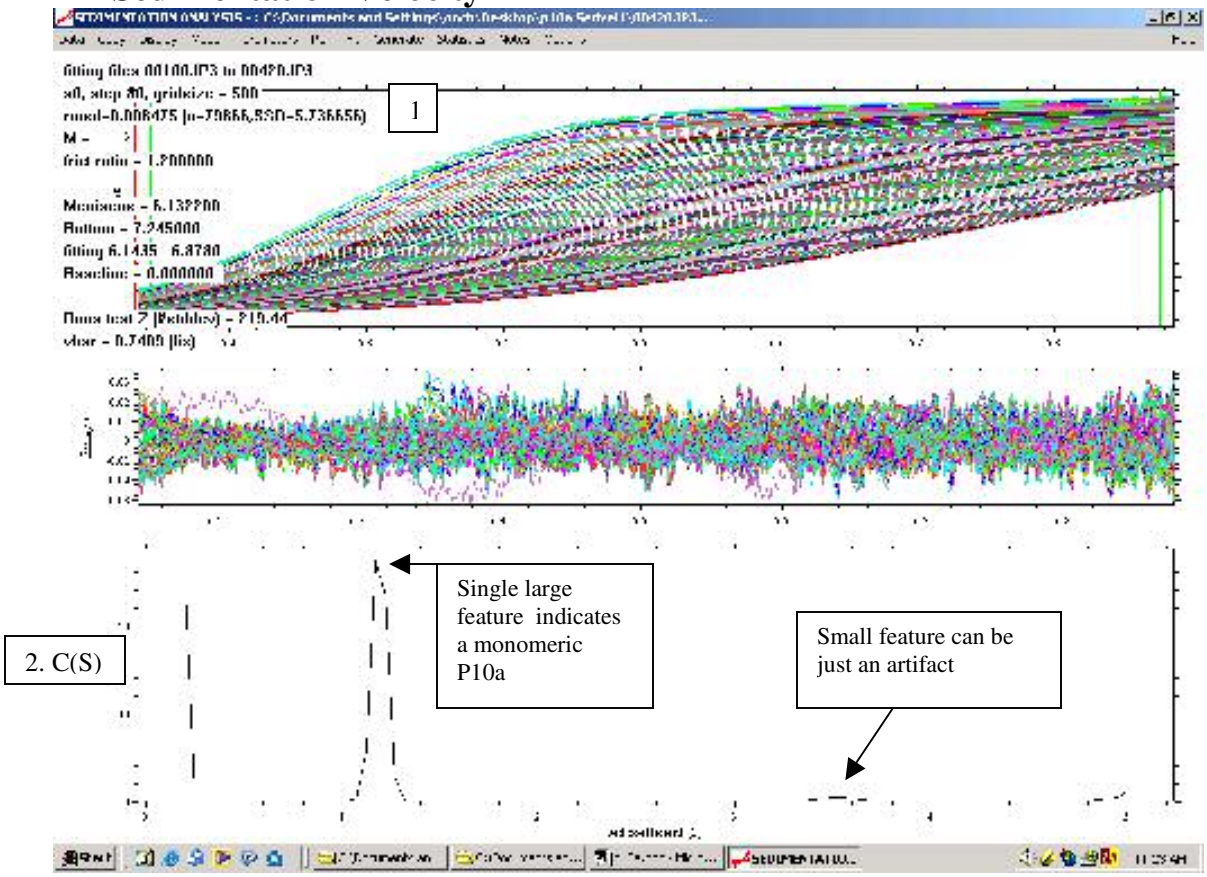

1. An initially uniform solution of p10a with buffer was placed in the cell and high angular velocity was used (55,000K) to cause rapid sedimentation of p10a toward the cell bottom. The boundary between depleted p10a concentration region near the meniscus and its sedimenting region was analyzed. The only one sharp sedimenting boundary indicates uniform concentration of solution and it suggests the homogeneity of solution, therefore, p10a is a monomer. **2.** The single large feature at 1.2S of the C(S) graph indicates a monomeric p10a. And a small feature at 3.5S can be interpreted in three possible ways. 1) The p10a exists mostly monomeric state, and a small portion of dimer and the interconversion between monomer and dimer is slow (two peaks are separated), 2) A small amount of aggregation was observed, or 3) It is also possible that it is just an artifact.

Figure 8

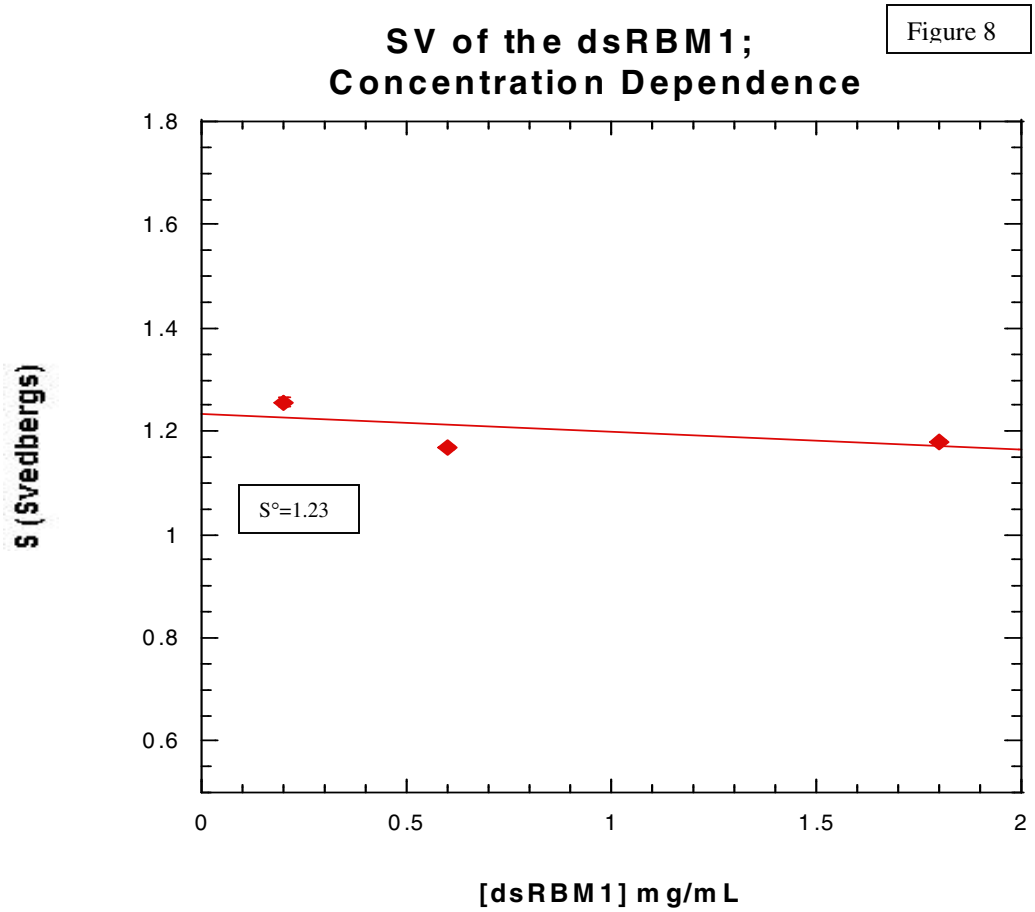

The sedimentation coefficient decreased slightly as protein concentration increased. The slight decrease in S with concentration is due to the hydrodynamic non-ideality. There is no self-association. The calculated sedimentation constant at zero concentration at 20 °C in water was 1.23 and its friction coefficient was 3.575×10^{-8}. Therefore, the frictional ratio is 1.30. The dsRBM I must be non-globular and have more asymmetric shape.

$S^\circ_{20,W} = S^\circ(1-\nu\rho_{20,W})\cdot\eta_{20,B} / (1-\nu\rho_{20,B})\cdot\eta_{20,W}$, $S^\circ = (1.23)\{(1 - .7409 \times .9982)(1.01\times10^{-2}) / (1-.7409\times1.00359)(1.002\times10^{-2})\}$ = **1.23**

$R^o = (3M\nu / 4\pi N_A)^{1/3}$, $R^o = \{(3\times10165.65\times.7409) / (4\pi\times6.022X10^{23})\}^{1/3} = 1.44\times10^{-7}$

$f^\circ = 6\pi\eta_{20,B}R^\circ$, $f^o = 6\pi(1.01\times10^{-2})(1.44\times10^{-7}) = 2.14\times10^{-8}$

$f_P = M(1-\nu\rho_{20,B}) / N_A\, S^\circ(1\times10^{-13})$, $f_P = \{10165.65\times(1-.7049\times.9982)\} / (6.022\times10^{23})\times1.23(1\times10^{-13})$ = **3.575×10^{-8}**

$f_P / f^\circ = (3.575\times10^{-8}) / (2.741\times10^{-8})$ = **1.30**

4-2 RNA Binding Stoichiometry (Figure 9)

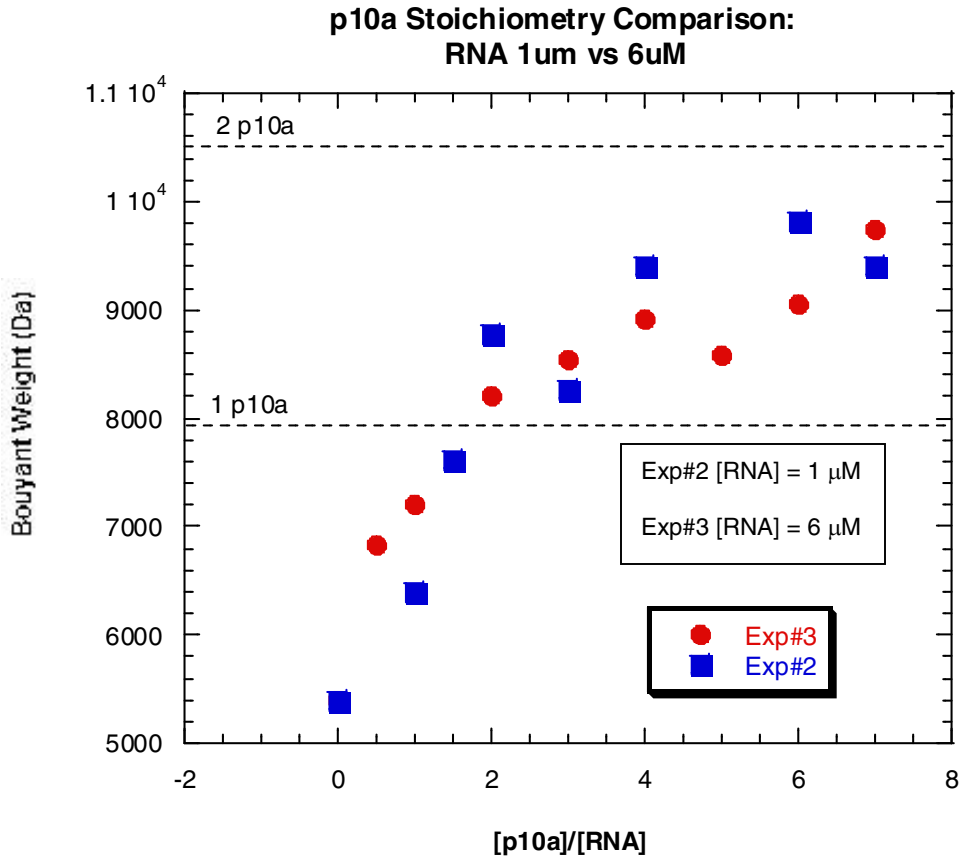

This graph shows two titration of a 20 base pair dsRNA with the dsRBM I (p10a). It was monitored by sedimentation equilibrium at 260 nm and 30,000 rpm. Under these conditions, the absorption contribution from the protein is negligible relative to the RNA because the extinction coefficient of RNA ($\varepsilon_{RNA,\ 260nm}$) is 50 times more then the extinction coefficient of p10a protein ($\varepsilon_{protein,\ 260\ nm}$). Therefore, as the number of protein that bound to dsRNA increases, the buoyant mass of the RNA also increases. The signal-average buoyant mass of the RNA in the absence of protein was 5385 in the 2nd experiment and 6930 in the 3rd experiment (theoretically 5944). The calculated buoyant mass of p10a is 2590 in analysis buffer. Over a protein concentration range of 0 to7 μM (#2) and 0 to 70 μM, M_{260} increased to approximately 9454. However, it did not reach to saturation. Therefore, it was not possible to determine its stoichiometry. It is probability due to a weak binding of p10a.

4-3 Nuclear Magnetic Resonance (NMR) (figure 10)

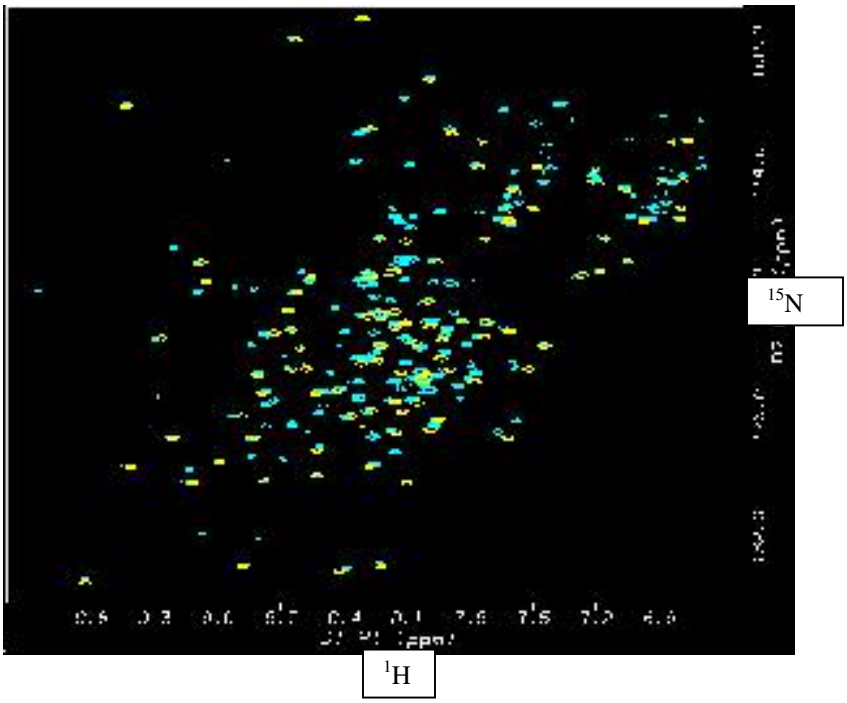

The overall folding of the p10a protein was assayed by NMR spectra. Protein enriched in ^{15}N was prepared growing cells in minimal medium containing ^{15}N-NH_4Cl as the labeled nitrogen source. The medium was prepared using and established protocol in Alexandrescu lab and enough ^{15}N p10a protein was produced for NMR analysis. In the spectrum (figure 13), the blue peaks are from dsRBD (p20) and yellow peaks are from dsRBM I (p10a). Since the yellow signals are at approximately the same position as blue signals (protein size and/or pH differences causes slight shifts) the overall folding of dsRBM I in p10a and p20 are the same.

4-4 Circular Dichroism Spectroscopy (Figure 11)

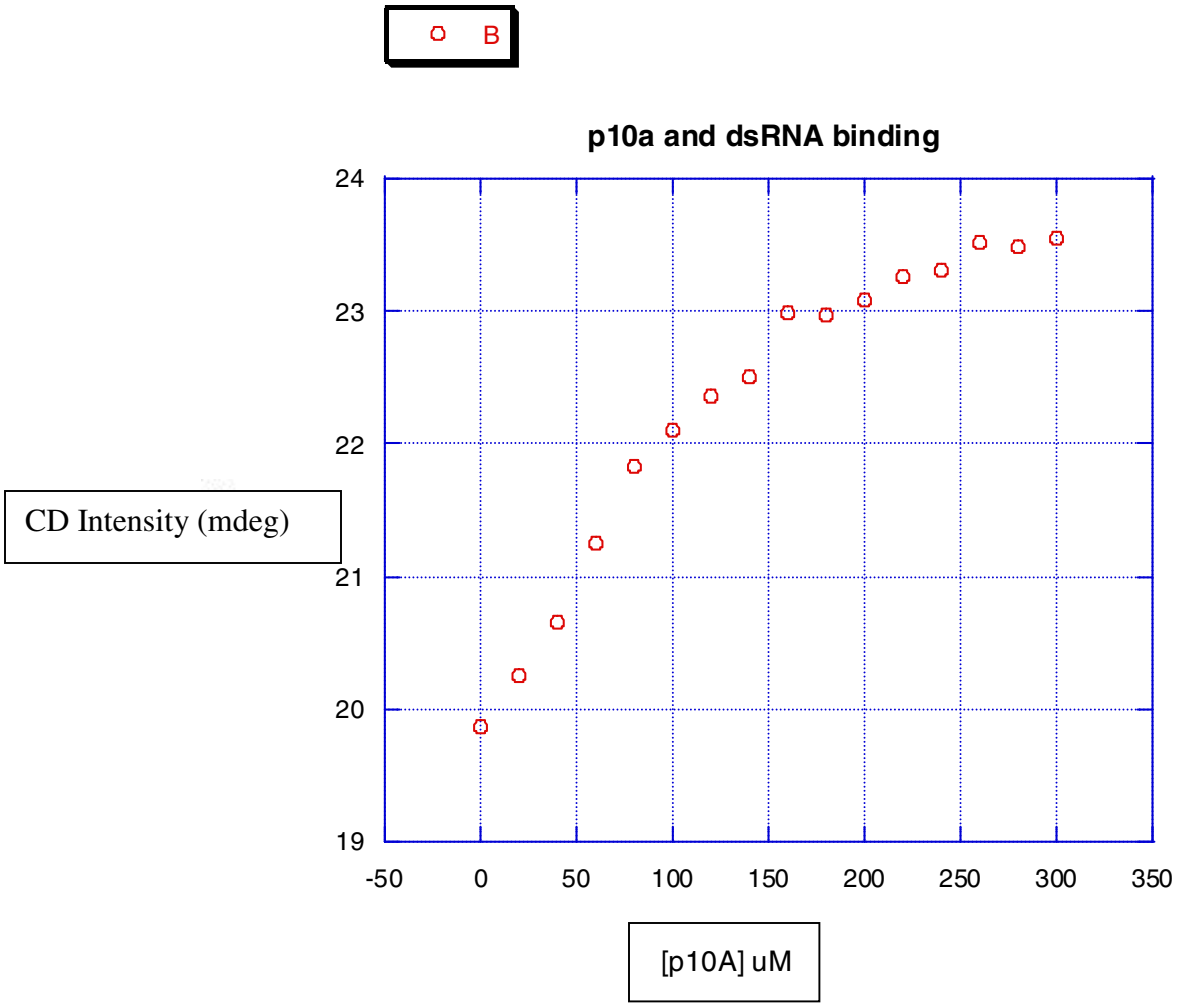

CD spectroscopy was also performed in order to determine the binding stoichiometry. In crystal structure of a related dsRBM, binding of the protein to dsRNA caused slight the unwinding the double helix (Ryter *et al.,* 1998) and the ellipticity near 260 nm is linearly related to the helical winding angle (Bloomfield *et al.,* 2000). Figure 10 shows a CD titration of the 20 base pair dsRNA with dsRBM I (p10a). It was performed at high RNA concentration (20 μM). Because these data show no saturation, the stoichiometry of p10a - 20mer dsRNA could not be determined.

5. Characterizing the binding of T16E p10a to a dsRNA

5-1 Mutagenesis - T16Ep10a

Through a search of the published sequence alignment of numerous dsRBMs of dsRNA binding proteins, the conserved sequences among the dsRBMs were found. A hypothesis was suggested that a mutation from threonine (polar) to glutamate (negatively charged) at position 16, which is consensus among many dsRBM include RNase III, would strengthen the bindings of p10a to dsRNA. Therefore, the introduction of a point mutation at T16E (ACA to GAA) was prepared.

The introduction of a point mutation was completed successfully. The transformation and digestion of the DNA went well. The numbers of colony on the plate were the following;

		Reaction 1	Reaction 2
+ DpnI	50 μL	6	6
	150 μL	20	44
	250 μL	10	45
- DpnI	150 μL	TNTC	TNTC

In order to confirm its sequence, ABI-Prism sequencing was performed and confirmed

5-2 Sedimentation equilibrium

The following two RNA binding stoichiometry graphs (Figure 12 and 13) show the result of several sedimentation equilibrium experiments of p10a-dsRNA binding under different conditions. In order to find its stoichiometry, several experiments were performed as trial and error to observe the saturation of their binding. The RNA binding stoichiometry I (Figure 12) is a graph of the binding comparison between mutant p10a T16E and wild type p10a to 1 μM and 20bp of dsRNA at 75 mM NaCl salt concentration.

Because p10a did not bind to dsRNA tightly, the saturation point was not observed. Therefore, salt concentration was lowered so that salts will not interact with the binding site of protein and RNA, hoping to create a better protein-RNA binding environment. The RNA binding stoichiometry II (Figure 12) shows the binding of p10a T16E to 1 μM and 20bp of dsRNA under the low salt concentration (10 mM NaCl). In order to observe the saturation, the second experiment was extended to the higher ratio of p10a T16E over RNA.

A mutation of threonine to glutamate was introduced at position 16 and the mutated p10a was set to bind to 20bp dsRNA under the low salt concentration. By combining the two changes (point mutation and salt concentration), the isolated p10a binding to dsRNA was observed up to saturation. This result supports the previously generated data three to one stoichiometry of dsRBD-dsRNA (Ucci, 2004). The modified salt condition is not the same as physiological condition; however, it is worth finding the binding stoichiometry and other character of binding mechanisms of PKR's motif.

RNA Binding Stoichiometry I (figure 12)

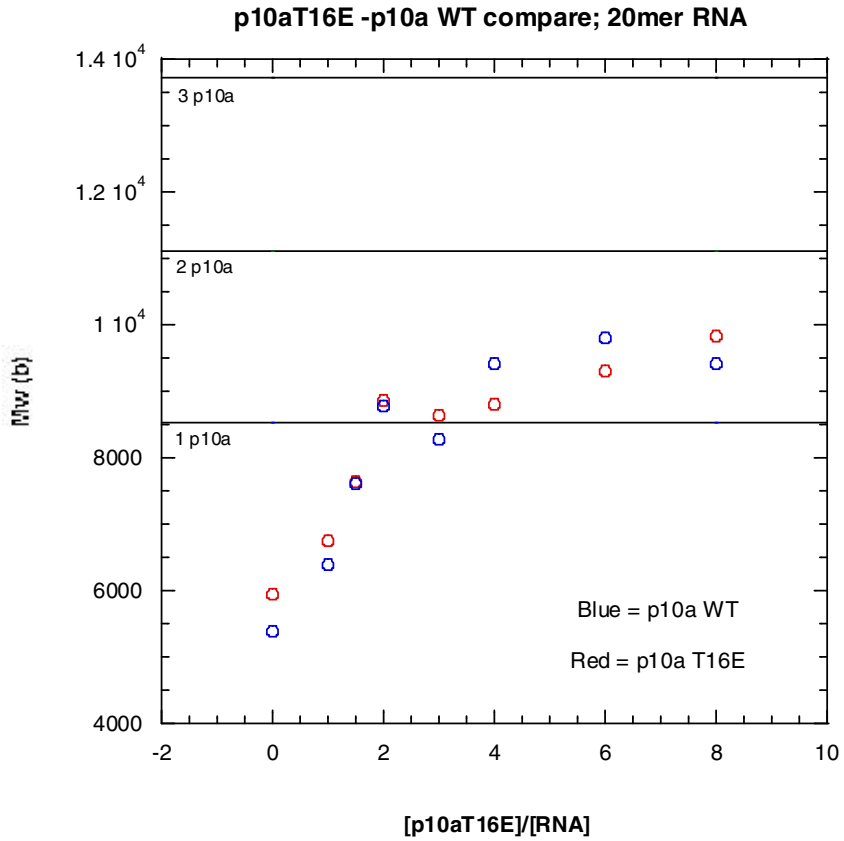

Sedimentation equilibrium was performed several times after the introduction of T16E mutation. If the mutation of one amino acid was significant enough to make protein's binding to dsRNA tighter, the graph should reach to saturation under such high dsRNA concentration. Figure 11 shows two titration of the 20bp dsRNA by wild type of dsRBM I (p10a WT, blue) and mutated dsRBM I (p10a T16E, red). In the comparison of these two motifs, M_{260} curves were similar and indicating the increase of binding of p10a to dsRNA. However, the buoyant molecule weight did not reach to the point of saturation. The mutationT16E alone did not help to bring their binding to saturation. Thus, the stoichiometry could not be determined

RNA Binding Stoichiometry II (Figure 13)

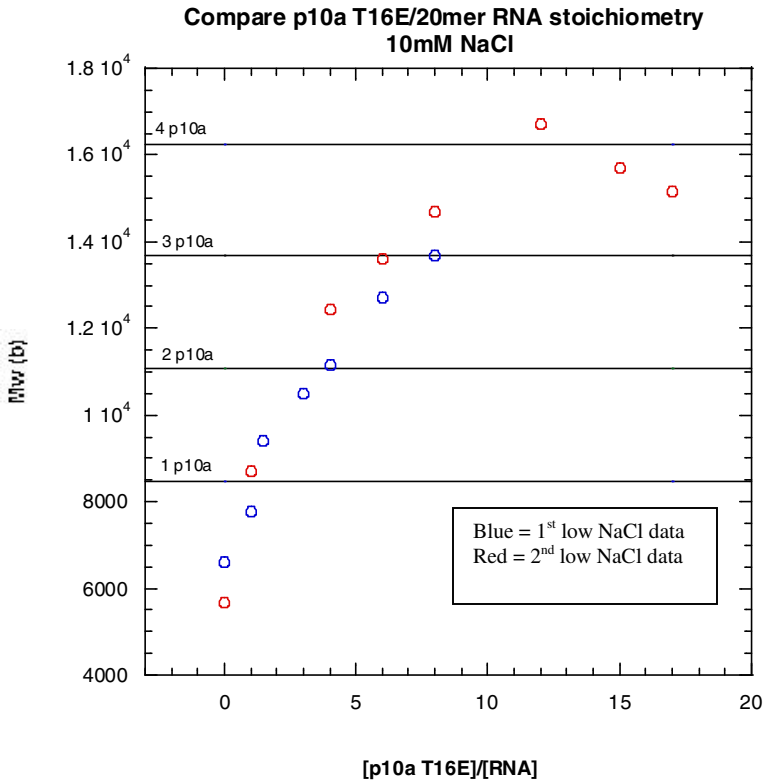

The sedimentation equilibrium data above shows saturation with three T16E p10a proteins bound to 20mer dsRNA under the low salt condition (10 mM NaCl). The mutation of T16E alone was not enough to make tighter binding of p10a to reach protein-dsRNA binding saturation. However, by lowering salt concentration to enhance binding of p10a to dsRNA, saturation was observed. In the first experiment, the p10a concentration was not high enough and saturation was not observed. Thus, for the second experiment, p10a the final concentration was increased from 8 μM to 17 μM and we were able to see a saturation point. This result of three to four dsRBM I binding to 20bp dsRNA agrees with Cole lab's stoichiometry result of dsRBD 20bp dsRNA (Ucci *et al.*, 2004).

Discussion

The dsRBMs play a key role in PKR function and regulation. Despite extensive investigation, their exact role in PKR activation is still not well understood. A detailed understanding of the mechanism of PKR activation is necessary to effectively target this enzyme for clinical intervention against cancer and viral infections. PKR is one of the most studied dsRNA binding proteins and I studied dsRBM I, one of the dsRBMs at the N terminus of PKR using biophysical approaches. A method of p10a expression in its native form was established as well as its purification method. My study of its binding characterization has produced fascinating results, which may overturn established theory. Further investigation on the subject will be necessary to confirm the findings.

1. p10a expression

A plasmid containing the dsRBM I gene (p10a) was received from Michael B. Mathews (New Jersey Medical School). The gene was in the pET-28 vector, containing an N-terminal polyhistidine tags, therefore, the gene needed to be transferred to pET-11a, non-histidine tag plasmid. These "tags" are fused to facilitate detection and purification of the target protein. However, the positively charged histidine tags may alter the structure and function of proteins. Thus, the native protein without tags was required in my research. The established protocol for purification of this protein was straightforward, only two columns were used and enough pure protein was harvested after the purification. Therefore, histidine tags are unnecessary.

The cloning and expressing of recombinant proteins in *E. coli* were performed using pET vectors (Novagen). Target genes were cloned in pET plasmids under control of strong bacteriophage T7 transcription, and expression was induced by providing a source of T7 RNA polymerase in the host cell. When the plasmid is transferred into an expression host containing a chromosomal copy of the T7 RNA polymerase gene under *lacUV5* control, the target protein was expressed upon the addition of IPTG to the bacterial culture. The design of pET vectors worked favorably with p10a gene, and high yield protein was harvested with a three-hour induction.

Transferring of p10a gene from pET-28 to pET-11a was attempted by two methods. One of the methods was double digestion of plasmids. Both plasmids, pET-28 with p10a gene and pET-11a, were first digested by the restriction enzymes, NdeI and BamHI. After digestion, the complementary ends of the digested DNA fragments were annealed, and sealed by treatment with DNA ligase. Because the selectable marker included on the vector was anmicillin resistance, only pET-11a containing the p10a gene was selected. Synthesis of the dsRBM I expression plasmid by site directed mutagenesis was performed as alternative method. A stop codon was inserted in the linker region between p10a (dsRBM I) and p10b (dsRBM II) using pET-11a-p20 made in Cole lab. Mutagenic primers were designed and the desired DNA was synthesized using the Quik-Change kit (Stratagene). In order to eliminate the methylated and non-mutated parent a DNA template, the PCR product was digested by DpnI. Since stop codon stops translation, only the p10a protein should be expressed.

Theoretically, both methods are feasible and wild type p10a protein was expected to be harvested. However, this stage was very time consuming and challenging. One of

the factors contributed to this difficulty could be the size of the protein. The p10a is a very small protein, it consists of only 91 amino acids, and therefore to recover this DNA from the gel was technically very difficult. After many trials, the double digestion and cloning method produced the p10a gene in a pET-11a vector. The product was transferred into XL1-Blue Supercompetent Cells.

Induction was tested by visualizing p10a expression with SDS-PAGE of whole cell lysate. A study of the time-course indicated that a three-hour induction yielded the maximum p10a protein (figure 3). Thus, three-hour induction was performed on a large scale in order to synthesize large quantity of p10a protein.

2. The p10a purification

The p10a protein purification method was adapted from a published p20 purification method (Ucci and Cole, 2004) with slight modifications. The buffer pH was decreased from pH 8.65 to pH 8.00, and the final sephacyl S-100 gel filtration was eliminated. At first, cell lysis was performed on cells suspended in buffer by sonication and PEI precipitation was performed in order to remove nucleic acid Protein in the supernatant was purified through a S-Sepharose ion exchange column followed by a Heparin Sepharose affinity column. The fractions monitored during S-Sepharose column purification showed a single large UV peak, indicating p10a protein elution, and a few UV peaks of contaminant (figure 4). The fractions of the p10a elution were visualized by the gel analysis and confirmed to be fairly purified protein with only few contaminants (figure 5). The p10a was diluted two-fold with buffer in order to reduce salt

concentration and was further purified through a Heparin Sepharose column equilibrated in buffer A. The p10a protein eluted at 250 mM NaCl without any contaminant (figure 6); therefore, this process resulted in p10a protein purification. The establishment of this purification method was straightforward and fewer steps were required. NMR was utilized to confirm folding of the isolated dsRBM I. Since protein folding is very important for protein's function, the confirmation of protein folding was important. The NMR indicated that the overall folding of both dsRBD (p20) and dsRBM I (p10a) were the same by overlapping signals of both proteins.

3. The P10a binding to dsRNA characteristics

Analytical ultracentrifugation is a useful tool for the detailed characterization of protein and for understanding the stoichiometry of protein-RNA interaction in free solution. Since PKR-RNA binding may have non-specific interactions, which generally have lower affinity and higher dissociation rates than specific interactions, it is particularly susceptible to artifacts associated with dissociation during the measurement. Solution equilibria may be defined by the gel shift and filter-binding assays under carefully controlled conditions; however, to achieve correct solution equilibria is meticulous process due to low affinity and high dissociation rates. Analytical ultracentrifugation provides more accurate characterization of dsRBM I-RNA interaction. The Cole lab has adapted a model for non-specific protein-RNA interaction for global fitting of multiwavelength sedimentation equilibrium analysis (Ucci and Cole, 2004). For the study of the mechanism of activation PKR by RNA binding, it is important to understand the interaction thermodynamics of various PKR domains with a structurally

defined dsRNA sequence. The multiwavelength sedimentation equilibrium is a practical method to characterize the stoichiometry and affinity of protein –nucleic acid interactions. The sedimentation equilibrium study does not require labeling of the reagents and uses fairly small amounts of material and measures the sequential binding of each protein ligand to the lattice. Thus, the relationship between sequential binding constants can be determined.

The sedimentation velocity was the first analysis performed in characterization of p10a protein. In sedimentation velocity experiment, a buffer diluted p10a sample, which was initially uniformly distributed, was placed in the cell and high angular velocity was used to cause relatively rapid sedimentation of p10a towards the cell bottom. As p10a was sedimenting towards the cell bottom, an evidence of homogeneity was observed by a single boundary. This result suggested that p10a protein existed as monomer in a free solution. In addition, C (S) analysis showed a single large feature at 1.2S, which indicated monomeric p10a. There was a very small feature at 3.0S, which may be explained by the presence of a small amount of dimeric p10a with a very slow interconversion rate. However, it was probably not the case because the sedimentation coefficient of 3.0S is too high to a dimer relative to the monomer peak at 1.2S. The dimer peak should appear about 1.5 times of the monomer peak. It may also be explained by the presence of very small amount of aggregate, or it can be just an artifact. Numerous studies have demonstrated dimerization of isolated binding motifs. Published data suggest that both dsRBMs have an intrinsic ability to dimerize (dsRBM II) or multimerize (dsRBM I) (Tian and Mathews, 2000). In contrast, my data indicated a monomeric state of dsRBM I in free solution and it contradicts the published data.

Further investigation is required to confirm my observation. The calculated sedimentation coefficient at zero concentration at 20°C in water was; $S°_{20,W} = 1.23$. The frictional coefficient of a smooth sphere model with the same molecular weight and specific volume of p10a is; $f° = 2.741 \times 10^{-8}$. And measured friction coefficient of p10a was; $f_{p10a} = 3.575 \times 10^{-8}$. Therefore, fractional ratio $f_{p10a} / f°$ was 1.30, indicating non-globular and asymmetric shape of p10a.

Sedimentation Equilibrium was also performed in order to characterize dsRBM I-dsRNA interaction. This experiment was a measurement of the increase in the buoyant mass of dsRNA up to saturation. If dsRBM I (p10a protein)-dsRNA interaction had reaches saturation, its stoichiometry could have been determined. However, to set conditions so that the interaction would reach saturation was difficult due to a very weak affinity of isolated p10a protein. A set of sedimentation equilibrium experiments was performed at dsRNA and p10a concentration. Regardless of my effort, wild type p10a did not bind tight enough to reach saturation. Therefore, mutations were introduced to control the protein-dsRNA binding strength by altering its amino acid side chain, T16E. This mutation was designed by locating conserved amino acids among tight binding dsRBMs. However, this mutation did not show any change in their affinity. An additional modification, lowering salt condition, was applied. Finally, protein-dsRNA binding reached saturation by introducing both modifications, thus its stoichiometry was determined as three or four to one (figure 12). This stoichiometry is the same as p20 and suggests that only dsRBM I binds to dsRNA. Therefore, a new overlapping lattice model of dsRBD-RNA binding, which Cole lab had introduced, was supported by my data as well.

Circular dichroism spectroscopy was also attempted to generate supporting data. To balance the protein and dsRNA concentration in order to obtain saturation was again a problem in this experiment. Despite several experiments by varying each concentration, the stoichiometry was not able to be determined yet. If the CD data agrees with the stoichiometry of protein-dsRNA interaction from the sedimentation results, it would be a very strong evidence to support the Cole lab's new overlapping lattice model.

References

1. Bloomfield, V.A, Crothers, D.M., Tinocco, I. (2000) Nucleic Acids: structures, properties and functions. *University Science Books.*
2. Carlson, C. B., Stephens, O. M. and Beal P. A. (2003) Recognition of Double-Stranded RNA by Proteins and Small Molecules. *Biopolymers* **70**, 86-102.
3. Conrad, C, Evguenieva-Hackenberg, E, Klug, G. (2001) Both N-terminal catalytic and C-terminal RNA binding domain contribute to substrate specificity and cleavage site selection of RNase III *FEBS Lett* **509**,53-58.
4. Fierro-Monti, I.and Mathews, M. B. (2000) Proteins binding to duplexed RNA: one motif, multiple functions. *Trends Biochem.* **25**, 241-246.
5. Gale, M., Jr., and Katze, M. G. (1998) Molecular mechanisms of interfereon resistance mediated by viral-directed inhibition of PKR, the interferon-induced protein kinase. *Pharmacol.,* **78**, 29-46
5. Joklik, Wolfgang, *et al.* (1998) *Zinsser Microbiology 19th ed.*
6. Lemaire, P. A., Lary, J., Cole, J. L. (2005) Mechanism of PKR Activation: Dimerization and Kinase Activation in the Absence of Double-stranded RNA. *J. Mol. Biol.* **345**, 81-90
7. Patel, R. C, Stanton, P. and Sen, G. C. (1996) Specific mutations near the amino terminus of double-stranded RNA-dependent protein kinase (PKR) differentially affect its double-stranded RNA binding and dimerization properties. *J. Biol. Chem.* **271**, 25657-25663.
8. Ryter, J. M., Schultz S. C. (1998) Molecular basis of double-stranded RNA-protein interactions: structure of a dsRNA-binding domain complex with dsRNA. *EMBO J*. **17**, 7505-7513.
9. Schmedt, C., Green, S. R., Manche, L., Taylor, D. R., Ma, Y., Mathews, M. B. (1955) Functional Characterization of the RNA-binding Domain and Motif of the Double-stranded RNA-dependent Protein Kinase DAI(PKR) *J. Biol. Chem.* **249,** 29-44
10. Spanggord, R. J., Vuyisich, Momchilo., Beal., P. A., (2002) Identification of Binding Sites for Both dsRBMs of PKR on Kinase-Activation and Kinase-Inhibiting RNA Ligands. *J. Biol. Chem.* **41**, 4511-4520.
11. Stark, G. R., Kerr, I. M., Williams, B. R., Silverman, R. H., Schreiber, R. D. (1998) How cells respond to interferons. *Annu, Rev. Biochem.* **67,** 227-264
12. Tian, B. and Mathews, M. B. (2001) Functional Characterization of and Cooperation between the Double-stranded RNA-binding Motifs of the Protein Kinase PKR. *J. Biol. Chem.* **13**, 9936-9944.
13. Ucci, J. W., Cole, M. L. (2004) Global analysis of non-specific protein-nucleic interactions by sedimentation equilibrium. *Biophysical Chem.* **108,** 127-140.

Research Advisor: _____

Dr. James L. Cole

Honors Advisor: _____

Dr. Lawrence Hightower